A Generalized Flux-Corrected Transport Algorithm I: A Finite-Difference Formulation

William J. Rider and Dennis R. Liles
Reactor Design and Analysis Group
Los Alamos National Laboratory
Los Alamos, NM 87545

Classification Index Numbers: 65M05, 76N10
Keywords: flux-corrected transport, conservation laws, high-resolution

Abstract

This paper presents a generalized flux-corrected transport (FCT) algorithm, which is shown to be total variation diminishing under some conditions. The new algorithm has improved properties from the standpoint of use and analysis. Results show that the new FCT algorithm performs better than the older FCT algorithms and is comparable with other modern methods. This reformulation will also allow the FCT to be used effectively with exact or approximate Riemann solvers and as an implicit algorithm.

1 Introduction

Godunov [1] showed that the monotonic solution of first- order hyperbolic conservation laws is at most first-order accurate for linear differencing schemes. The first algorithm to successfully address this difficulty was the flux-corrected transport (FCT) algorithm of Boris, Book, and Hain![2, 3, 4, 5] . This algorithm performed quite well on linear advection problems and paved the way for future developments in the field. It essentially consisted of computing a solution with a nondiffusive transport method followed by a stabilizing diffusive step. This monotone solution is then used to aid in the construction of an antidiffusive step in which the solution from the first part of the algorithm is locally sampled and corrections are "patched" to it. This is accomplished with a flux limiter that only applies the flux corrections in the smooth part of the flow. As a result, the solution will be of a high-order in smooth parts of the convected profile, but first-order near discontinuities and steep gradients. Extension of the FCT algorithm to systems of conservation laws, however, has proved less successful.

Further developments on this topic were achieved by van Leer [6] in his higher order extensions of Godunov's method often referred to as MUSCL. The prescription of slope-limiting used by van Leer has great similarity to the flux-limiting used in the original FCT. The difficulties associated with FCT with systems equations is not shared by MUSCL because an exact or approximate solution to the local Riemann problem is used to construct the convective fluxes. While this approach adds complexity and cost to the solution procedure, the corresponding quality of the solution is greatly improved. Recently, researchers have extended the ideas of van Leer to arbitrarily high-order spatially or temporally and christened these methods as uniformly [7] or essentially [8] nonoscillatory (UNO or ENO) schemes.

The effort to put the new modern algorithms on firmer theoretical footing resulted in the concept of total variation diminishing (TVD) methods [9], which have a number of desirable properties. To be total variation diminishing, a scheme must satisfy the following inequalities,

$$TV\left(u^{n+1}\right) \leq TV\left(u^{n}\right) \ ,$$

where

$$TV\left(u\right) = \sum_{j=-\infty}^{\infty} \left|u_{j+1} - u_{j}\right| \ .$$

While these methods include classic monotone schemes, they can also be extended to include methods that are second-order in the L_1 norm. By construction, these methods are still first-order at points of extrema (in the L_∞ norm). A second property of TVD schemes, which is both useful and satisfying, is that they can be extended to include implicit temporal differencing [10]. This generality is quite desirable as it allows a more general use of TVD algorithms for a wide range of problems. It should be noted that MUSCL schemes have also been extended to include implicit temporal differencing [11, 12].

Zalesak [13] redefined the FCT in such a way as to make it more general. A standard low-order solution, similar to that obtained by donor-cell differencing, is used to define a monotonic solution. This solution is then used to limit an antidiffusive flux, which is defined as the difference between a high-order and low-order flux. As with the earlier versions of the FCT, the limiter is designed to give no antidiffusive flux when an extrema or a discontinuity is reached. This prescription of the FCT can allow the user to specify a wide range of low-order fluxes as well as a large variety of high-order fluxes. These have included central differencing of second or higher order, Lax-Wendroff, and spectral fluxes [14]. Recently, several researchers [15] have introduced an implicit FCT algorithm; however, this algorithm is limited to small multiples of the Courant-Friedrichs-Lewy (CFL) number. This is because the low-order solution is produced by multiple sub-cycles with an explicit donor-cell (or other monotonic) solution and an implicit high-order solution. The high-order solution is only stable for small multiples of the CFL number, thus limiting the applicability of this algorithm. The FCT has also been extended for use with a finite-element solution method with great success [16].

The performance of the explicit FCT algorithm is the subject of this paper. Several investigators [17] [18] have noted for the older FCT algorithm that a lower CFL limit is required for stability. The FCT algorithm also suffers from being overcompressive (as will be shown in Section 3). This was shown in a test of the FCT on a shock tube problem [19], where even at a CFL number of 0.1, the solution was of relatively poor quality. This probably is due to the handling of the pressure-related terms in the momentum and energy equations. This work aims to address these problems, first through making several improvements to the FCT and then by showing the extension of this modified FCT to systems of equations. In accomplishing this, we will make extensive use of approximate Riemann solvers of the type introduced by Roe [20].

We have several objectives to be addressed in this paper: the performance of FCT on systems of equations, which needs to be improved in terms of solution quality, and efficiency (the necessity of using small CFL numbers), more direct ties to other modern algorithms (such as TVD algorithms), and analysis of the potential TVD properties of FCT methods. The first objective will follow the last two objectives in treatment. The first two objectives are complementary in nature and should follow from one another. In producing new FCT algorithms, we will seek one step methods, not requiring the diffusive first step used in older FCT methods.

This paper is organized into four sections. The following section provides an overview of the numerical solution of hyperbolic conservation laws. Later in that section, the FCT method according to Zalesak is introduced. This method is analyzed and suggestions for improvements are made including the extension of FCT to systems of equations. This takes two forms: one method is denoted as the "new FCT" method, and the second is denoted as the "modified-flux FCT" method. The "new FCT" method is similar to symmetric TVD methods, and the "modified-flux FCT" is similar to Harten's modified-flux TVD method. In the third section, results are presented for the methods discussed in the paper. These results are for a scalar wave equation, Burgers' equation and a shock tube problem for the Euler equations. Finally, some closing remarks will be made.

2 Method Development

Before describing the changes we will make in the FCT algorithm, we will make several introductory points. Consider

$$\frac{\partial u}{\partial t} + \frac{\partial f\left(u\right)}{\partial x} = 0 \; , \tag{1}$$

which is a first-order hyperbolic transport equation for u where f is the flux of u. Equation (1) can be written as

$$\frac{\partial u}{\partial t} + a\frac{\partial u}{\partial x} = 0 \; , \tag{2}$$

where

$$a = \frac{\partial f}{\partial u} \; .$$

The characteristic speed, a, is particularly useful in defining finite-difference solutions to Eq (1). A system of conservation laws can be similarly defined; however, the construction of effective finite-difference solution for systems of equations requires more care. Consider

$$\frac{\partial \mathbf{U}}{\partial t} + \frac{\partial \mathbf{F}\left(\mathbf{U}\right)}{\partial x} = 0 \; , \tag{3}$$

which is a set of hyperbolic conservation laws where $\mathbf{U}$ is a column vector $\left(u^1, u^2, \ldots, u^m\right)^T$ of conserved quantities and $\mathbf{F}\left(\mathbf{U}\right)$ is a column vector $\left(f^1, f^2, \ldots, f^m\right)^T$ of fluxes of $\mathbf{U}$. Equation (3) can be written as

$$\frac{\partial \mathbf{U}}{\partial t} + A\frac{\partial \mathbf{U}}{\partial x} = 0 \; , \tag{4}$$

where

$$A = \frac{\partial \mathbf{F}\left(\mathbf{U}\right)}{\partial \mathbf{U}} = \left[\begin{array}{ccc} \partial f^1/\partial u^1 & \ldots & \partial f^1/\partial u^m \\ \vdots & \ddots & \vdots \\ \partial f^m/\partial u^1 & \ldots & \partial f^m/\partial u^m \end{array} \right] \; .$$

The matrix A is the flux Jacobian for the system defined by Eq. (3), which is quite useful in the construction of finite-difference solutions of this system of equations, as will be shown in Section 2.4 of this paper.

In general, equations of the type considered above can develop discontinuous solutions even when the initial data is smooth. Because of this, the solutions are not unique. To rectify this, the admissible solutions must satisfy an entropy condition (for details on this see [21] [22]). It is the formation of discontinuities in the solution that causes the difficulties for finite-difference solutions of Eq. (1). At these discontinuities, the function ceases to be smooth and the usual assumptions made in constructing finite-difference approximations collapse. As a result, more physical information needs to be incorporated into the solution procedure.

The FCT (and most other finite-difference methods) was constructed to solve Eq. (1). This approach will be followed initially, but will eventually be abandoned to some extent when systems of equations are considered. First, the basics of Zalesak's FCT will be reviewed, followed by several basic suggestions for improvements in this algorithm. These improvements will be discussed briefly with comparisons being drawn between these new FCT methods and the symmetric TVD schemes [23]. Finally, the FCT will be extended to systems of hyperbolic conservation laws using an approximate Riemann solver.

For the remainder of the presentation, the following nomenclature will be used: $\Delta_{j+\frac{1}{2}} u = u_{j+1} - u_j$. A conservative finite-difference solution to Eq. (1) using a simple forward Euler time discretization is

$$u_j^{n+1} = u_j^n - \lambda \left(\hat{f}_{j+\frac{1}{2}} - \hat{f}_{j-\frac{1}{2}} \right) \ , \tag{5}$$

where $\lambda = \Delta t / \Delta x$. The temporal spacing is Δt and Δx is the spatial mesh spacing that will be assumed constant for the remainder of the paper (varying mesh widths will result is somewhat more complex expressions). The superscript n refers to time, $n+1$ refers to the time $t + \Delta t$, and the subscript j refers to space with j being a cell center and $j \pm \frac{1}{2}$ being the cell edges. The construction of the numerical fluxes $\hat{f}_{j\pm\frac{1}{2}}$ will be the subject of this section. The cell edge flux is defined as

$$\hat{f}_{j+\frac{1}{2}} = \frac{1}{2} \left(f_j + f_{j+1} \right) + \phi_{j+\frac{1}{2}} \ , \tag{6}$$

where ϕ is a numerical dissipation term. For a system of equations the flux is written

$$\hat{\mathbf{F}}_{j+\frac{1}{2}} = \frac{1}{2} \left(\mathbf{F}_j + \mathbf{F}_{j+1} \right) + \Phi_{j+\frac{1}{2}} \ , \tag{7}$$

where $\mathbf{F}$ and Φ are vectors, but are defined similarly to the single equation case. For instance, the first-order donor-cell flux is

$$\hat{f}^{DC}_{j+\frac{1}{2}} = \frac{1}{2}\left(f_j + f_{j+1} - \left|a_{j+\frac{1}{2}}\right| \Delta_{j+\frac{1}{2}} u\right) \ , \tag{8}$$

thus

$$\phi^{DC}_{j+\frac{1}{2}} = -\frac{1}{2}\left|a_{j+\frac{1}{2}}\right| \Delta_{j+\frac{1}{2}} u \ .$$

For the remainder of the paper, the prescription of the numerical dissipation term, ϕ or Φ, will be used to define algorithms. One slight modification of the above methodology is used for nonlinear equations and systems; as suggested by Yee [23] an entropy fix is implemented for the donor-cell differencing, which modifies the use of the absolute value in donor-cell differencing of a characteristic speed, by

$$\psi(z) = \begin{cases} |z| & \text{if } |z| \geq \epsilon \\ \left(z^2 + \epsilon^2\right)/2\epsilon & \text{if } |z| < \epsilon \end{cases} \ , \tag{9}$$

if one is dealing with a linear equation set $\epsilon = 0$. The parameter ϵ is determined by the following equation [24],

$$\epsilon = \max\left[0, a_{j+\frac{1}{2}} - a_j, a_{j+1} - a_{j+\frac{1}{2}}\right] \ .$$

Thus, the numerical diffusion term in the donor-cell flux becomes

$$\phi^{DC}_{j+\frac{1}{2}} = -\frac{1}{2}\psi\left(a_{j+\frac{1}{2}}\right) \Delta_{j+\frac{1}{2}} u \ .$$

This description of the donor-cell method reduces to Roe's method [20] for scalar equations. The term donor-cell methods and Roe's methods should be viewed as equivalent in this sense.

2.1 Zalesak's FCT Algorithm

Zalesak's FCT has been classified as a hybrid method that is applied in two steps. By being hybrid, the algorithm is based on the blending of high- and low-order difference schemes together. Step one is accomplished with a first-order monotonic solution such as donor-cell plus some additional diffusion (the entropy fix discussed in the previous section adds such dissipation). This could be accomplished with other first-order algorithms such as Godunov's [1] or Engquist and Osher's [25]. These fluxes are used to produce a transported diffused solution $\tilde{u}$ as follows:

$$\tilde{u}_j = u^n_j - \lambda\left(\hat{f}^{DC}_{j+\frac{1}{2}} - \hat{f}^{DC}_{j-\frac{1}{2}}\right) \ . \tag{10}$$

A high-order flux, f^H, is defined in some way and then the low-order flux is subtracted from the high-order flux to define the antidiffusive flux as

$$\hat{f}^{AD}_{j+\frac{1}{2}} = \hat{f}^{H}_{j+\frac{1}{2}} - \hat{f}^{L}_{j+\frac{1}{2}} \ ,$$

where in this paper, we have defined $\hat{f}^L = \hat{f}^{DC}$. The antidiffusive flux is then limited with respect to the local gradients of the conserved variable computed with the transported and diffused solution. Zalesak defined his limiter as a prelude to a truly multidimensional limiter, but also defined an equivalent limiter as

$$\hat{f}^{C}_{j+\frac{1}{2}} = S_{j+\frac{1}{2}} \max\left\{0, \min\left[S_{j+\frac{1}{2}}\lambda^{-1}\Delta_{j-\frac{1}{2}}\tilde{u}, \left|\hat{f}^{AD}_{j+\frac{1}{2}}\right|, S_{j+\frac{1}{2}}\lambda^{-1}\Delta_{\frac{3}{2}}\tilde{u}\right]\right\} \ , \quad (11)$$

where $S_{j+\frac{1}{2}} = \hat{f}^{AD}_{j+\frac{1}{2}} / \left|\hat{f}^{AD}_{j+\frac{1}{2}}\right|$ is the sign of the conserved variable's gradient spatially. This limiter is identical to the limiter defined by Boris and Book [2], but with a different definition of $\hat{f}^{AD}$. The final cell-edge numerical diffusion is defined by

$$\phi^{FCT}_{j+\frac{1}{2}} = \hat{f}^{C}_{j+\frac{1}{2}} + \phi^{DC}_{j+\frac{1}{2}} \ . \quad (12)$$

The FCT generally carries a stability limit on its time step of

$$\lambda \left|a\right| \leq 1 \ .$$

Before going further, several critical comments need to be made concerning this algorithm. Despite the striking generality, which is driven by the prescription of the antidiffusive fluxes, the algorithm has some deficiencies. By its formulation as a two-step method it has some disadvantages in terms of analytical analysis and efficiency of implementation. By the use of the inverse grid ratio λ^{-1} in the flux limiter, the algorithm is effectively limited to explicit time discretization (as will be shown in the following section). The use of a diffused solution in the limiter is important in stabilizing the solution, which could yield oscillatory solutions without this step. Under closer examination, the use of a diffused solution acts as an upwind weighted artificial diffusion term. This sort of definition could lead to a fairly complex one-step FCT algorithm, which has, at first glance similarity to UNO-type schemes. The diffusive terms in the FCT algorithm's limiter are upwind weighted rather than centered as with UNO based algorithms. This can be seen by direct substitution of the diffusive first step into the second step of the algorithm. Additionally, numerical experiments with a scalar advection equation show that the total variation for the FCT solution can increase with time for a CFL number less than one.

The use of higher order antidiffusive fluxes with this prescription of the FCT also raises some questions about the actual order of the approximation. The antidiffusive flux is of the higher order, but the local gradients in the limiter are only accurate to second-order. This suggests that the solution may actually be of only second-order spatially (in the L_1 norm). This also holds for temporal order as the local gradient terms are only first-order in space, thus an antidiffusive flux based on a Lax-Wendroff flux may actually yield a first-order accurate temporal approximation. Thus the form of the local gradients used in the limiter may also need to be modified to accomplish the goal of true higher order accuracy.

This seems to contradict results reported in [26, 27], but these results are for a scalar wave equation where the solution is translated by the flow field. With nonlinear equations or systems this may cause difficulties because of the formation of shocks and discontinuities. This is explored further in Section 3.2.

2.2 A New FCT Algorithm

The first and simplest change is to rewrite the flux limiter as

$$\hat{f}^{C}_{j+\frac{1}{2}} = S_{j+\frac{1}{2}} \max\left\{0, \min\left[S_{j+\frac{1}{2}}\tilde{\sigma}_{j-\frac{1}{2}}\Delta_{j-\frac{1}{2}}\tilde{u}, \left|\hat{f}^{AD}_{j+\frac{1}{2}}\right|, S_{j+\frac{1}{2}}\tilde{\sigma}_{j+\frac{3}{2}}\Delta_{j+\frac{3}{2}}\tilde{u}\right]\right\} , \tag{13}$$

where

$$\tilde{\sigma}_{j+\frac{1}{2}} = \psi\left(\tilde{a}_{j+\frac{1}{2}}\right) , \tag{14}$$

or

$$\tilde{\sigma}_{j+\frac{1}{2}} = \psi\left(\tilde{a}_{j+\frac{1}{2}}\right) - \lambda\tilde{a}^{2}_{j+\frac{1}{2}} , \tag{15}$$

and $S_{j+\frac{1}{2}}$ has the same definition as before. The second choice for $\tilde{\sigma}_{j+\frac{1}{2}}$ gives second-order accuracy in both time and space if $\hat{f}^{AD}_{j+\frac{1}{2}}$ is of similar or higher accuracy [9]. This relatively small change has a significant impact on the FCT algorithm as will be shown later both analytically and computationally. This form is also a great deal closer to the definition of limiters used in TVD algorithms. However, this still leaves a two-step method which poses some problems from the standpoint of efficiency and extension to systems of conservation laws.

The similarities of this modification of the FCT with symmetric TVD schemes [23] are quite strong. The necessary changes to convert this scheme into one equivalent to the one described by Yee are simple. This consists of dividing the local gradient terms in the limiter by two and removing the first step of the FCT. Yee writes the numerical flux for the symmetric TVD method as

$$\hat{f}_{j+\frac{1}{2}} = \frac{1}{2}\left[a_{j+\frac{1}{2}}\left(u_j + u_{j+1}\right) - \psi\left(a_{j+\frac{1}{2}}\right)\Delta_{j+\frac{1}{2}}u + Q_{j+\frac{1}{2}}\right] . \tag{16}$$

An example of the $Q_{j+\frac{1}{2}}$ function would be

$$\begin{aligned} Q_{j+\frac{1}{2}} = S_{j+\frac{1}{2}} \max\Big\{0, \min\Big[& S_{j+\frac{1}{2}} \quad \psi\left(a_{j+\frac{3}{2}}\right)\Delta_{j+\frac{3}{2}}u, \psi\left(a_{j+\frac{1}{2}}\right)\Delta_{j+\frac{1}{2}}u, \\ & S_{j+\frac{1}{2}} \quad \psi\left(a_{j-\frac{1}{2}}\right)\Delta_{j-\frac{1}{2}}u\Big]\Big\} , \end{aligned} \tag{17}$$

which strikes a strong resemblance with Eq. (13) for an antidiffusive flux defined with a second-order central difference. For ease of analysis, this method is rewritten in the following form:

$$\hat{f}_{j+\frac{1}{2}} = \frac{1}{2}\left[a_{j+\frac{1}{2}}\left(u_j + u_{j+1}\right) - \psi\left(a_{j+\frac{1}{2}}\right)\left(1 - Q_{j+\frac{1}{2}}\right)\Delta_{j+\frac{1}{2}}u\right] , \tag{18}$$

where

$$Q_{j+\frac{1}{2}} = \text{minmod}\left(1, r^{+}_{j+\frac{1}{2}}, r^{-}_{j+\frac{1}{2}}\right) ,$$

with $r^{+}_{j+\frac{1}{2}} = \Delta_{j+\frac{3}{2}}u/\Delta_{j+\frac{1}{2}}u$ and $r^{-}_{j+\frac{1}{2}} = \Delta_{j-\frac{1}{2}}u/\Delta_{j+\frac{1}{2}}u$. The minmod limiter used with symmetric TVD schemes is defined by Yee, but has the same effect as Eq. (17).

Theorem 1 *The new FCT algorithm without the monotone (TVD) first step is TVD under the following conditions: for $\tilde{\sigma} = \psi(a)$*

$$\lambda |a| < \frac{1}{2(1-\theta)} , \tag{19}$$

and for $\tilde{\sigma} = \psi(a) - \lambda a^2$

$$\lambda |a| < \frac{1}{1-\theta} . \tag{20}$$

Here θ is an implicitness parameter (see Yee [23]) with $\theta = 1$ the equation is fully implicit, and with $\theta = 0$ the equation is fully explicit. Without the monotone first step, the fully explicit old FCT algorithm is not TVD for any CFL number, but the implicit FCT algorithm is TVD under the condition

$$\lambda |a| < \frac{\theta}{1-\theta} . \tag{21}$$

Proof. The FCT cell-edge flux can be written in the same way as the flux for a symmetric TVD scheme by defining

$$\hat{f}^{C}_{j+\frac{1}{2}} = \frac{1}{2}\left|a_{j+\frac{1}{2}}\right| Q_{j+\frac{1}{2}}\Delta_{j+\frac{1}{2}}u \ , \tag{22}$$

if $Q_{j+\frac{1}{2}}$ is based on Eq. (14)

$$Q_{j+\frac{1}{2}} = \mathrm{minmod}\left(1, 2\tilde{r}^{+}, 2\tilde{r}^{-}\right) \ ,$$

and if $Q_{j+\frac{1}{2}}$ is based on Eq. (15)

$$Q_{j+\frac{1}{2}} = \left(1 - \lambda\left|a_{j+\frac{1}{2}}\right|\right) \mathrm{minmod}\left(1, 2\tilde{r}^{+}, 2\tilde{r}^{-}\right) \ ,$$

and

$$\tilde{r}^{+} = \frac{\Delta_{j+\frac{3}{2}}\tilde{u}}{\Delta_{j+\frac{1}{2}}u} \ ,$$

$$\tilde{r}^{-} = \frac{\Delta_{j-\frac{1}{2}}\tilde{u}}{\Delta_{j+\frac{1}{2}}u} \ .$$

In [23] the inequalities that need to be satisfied in order for a flux of the form given in Eq. (16) to be TVD are

$$Q_{j+\frac{1}{2}} < 2 \ , \tag{23}$$

and

$$\frac{Q_{j+\frac{1}{2}}}{r^{\pm}_{j+\frac{1}{2}}} < \frac{2}{\lambda\left(1-\theta\right)\left|a_{j+\frac{1}{2}}\right|} - 2 \ , \tag{24}$$

$$\lambda\left|a\right| < \frac{1}{1-\theta} \ . \tag{25}$$

The FCT limiter given in Eq. (13) satisfies the first and last of these relations, but satisfaction of the other relation (24) in a rigorous manner has proved to be more difficult. To establish some bounds on the properties of the FCT solutions, the first step of the FCT will be ignored for the time being. Given this, the worst cases for the limiter are $Q = 2r^{\pm}$ or $2\left(1-\lambda\left|a\right|\right)r^{\pm}$. Comparing the first of these cases with Eq. (24) gives

$$2 < \frac{2}{\lambda\left(1-\theta\right)\left|a\right|} - 2 \ ,$$

or

$$\lambda\,|a| < \frac{1}{2\,(1-\theta)}\ .$$

For the second of the two cases,

$$2\,(1-\lambda\,|a|) < \frac{2}{\lambda\,|a|\,(1-\theta)} - 2\ ,$$

or

$$\lambda\,|a| < \frac{1}{1-\theta}\ .$$

Remark 1 *Thus, even without the first step, the new FCT algorithm is TVD under some conditions (given above). Thus the implementations of this method should not include the diffusive first step because it is not necessary. It is also unconditionally stable for fully implicit temporal discretization. The first step adds more dissipation into the algorithm, which should result in higher CFL limits for the first case. Numerical experiments confirm this and show that the new FCT is TVD for all CFL numbers less than one.*

Zalesak's FCT can be subjected to a similar test after a reformulation of its limiter. Given the same definition as before for $f^C_{j+\frac{1}{2}}$,

$$Q_{j+\frac{1}{2}} = \text{minmod}\left(1, \frac{2\tilde{r}^+}{\lambda\,|a|}, \frac{2\tilde{r}^-}{\lambda\,|a|}\right)\ , \tag{26}$$

where $\tilde{r}^{\pm}$ are defined as before. Using Eq. (24), and again neglecting the first step, one can show that

$$\lambda\,|a| < \frac{\theta}{1-\theta}\ . \tag{27}$$

□

Remark 2 *Thus, for a fully explicit approximation without the first step, Zalesak's FCT is never TVD. However, as the degree of implicitness increases, the algorithm becomes TVD for some CFL numbers and eventually becomes unconditionally TVD at $\theta = 1$. If one looks at the form of the limiter as the CFL number increases, the effective antidiffusive flux reduces in an inversely proportional fashion. Therefore, at large CFL numbers, Zalesak's FCT is largely ineffective as a high-order implicit algorithm. Numerical experiments have shown that with the first step, Zalesak's FCT produces results that diminish in total variation up to a CFL number of about 0.95.*

The new FCT method given above is an analog to the symmetric TVD method. Another form of common TVD method is Harten's modified flux method. The next section describes a FCT method developed along those lines.

2.3 A Modified-Flux FCT Algorithm

To attain these goals, the FCT will be recast in the form of Harten's modified-flux TVD scheme [9]. From this basis several FCT limiters can be shown to be TVD by the criteria given by [28], and the FCT can be written as a one-step method and extended to use as an implicit algorithm in the same way as TVD methods are [10]. This will be examined in a future paper.

The modified-flux TVD method is defined by computing cell-centered modified fluxes and making the overall flux upwind with respect to both the "physical" and modified fluxes. Formally, the modified-flux formulation has a dissipation term,

$$\phi^{MF}_{j+\frac{1}{2}} = \frac{1}{2}\left[g_j + g_{j+1} - \psi\left(a_{j+\frac{1}{2}} + \gamma_{j+\frac{1}{2}}\right)\Delta_{j+\frac{1}{2}}u\right] , \tag{28}$$

where

$$g_j = \mathrm{minmod}\left(\sigma_{j-\frac{1}{2}}\Delta_{j-\frac{1}{2}}u, \sigma_{j+\frac{1}{2}}\Delta_{j+\frac{1}{2}}u\right) , \tag{29}$$

and

$$\gamma_{j+\frac{1}{2}} = \begin{cases} \dfrac{\Delta_{j+\frac{1}{2}}g}{\Delta_{j+\frac{1}{2}}u} & \text{if } \Delta_{j+\frac{1}{2}}u \neq 0 \\ 0 & \text{otherwise} \end{cases} . \tag{30}$$

The minmod function of two arguments has the usual definition given in [29], which gives the same effect as the FCT limiter for three arguments. A general form of the minmod function for two arguments is

$$\begin{aligned} \mathrm{minmod}\,(a,b;n) = \mathrm{sign}\,(a) \max\,[\,0,\quad & \min\quad (n\,|a|\,, \mathrm{sign}\,(a)\,b)\,, \\ & \min\quad (|a|\,, n\ \mathrm{sign}\,(a)\,b)\,]\ , \end{aligned} \tag{31}$$

which for $n = 2$ gives the Superbee limiter developed by Roe [30]. The function $\sigma_{j+\frac{1}{2}}$ can have several forms, including

$$\sigma_{j+\frac{1}{2}} = \frac{1}{2}\psi\left(a_{j+\frac{1}{2}}\right) , \tag{32}$$

or

$$\sigma_{j+\frac{1}{2}} = \frac{1}{2}\left[\psi\left(a_{j+\frac{1}{2}}\right) - \lambda a^2_{j+\frac{1}{2}}\right] . \tag{33}$$

For Eq. (32), the stability limit depends on the form of the limiter, for instance the general minmod limiter yields a stability limit of

$$\lambda\,|a| \leq \frac{2}{(2+n)\,(1-\theta)}$$

for $n \leq 2$. The use of Eq. (33) gives a stability limit of

$$\lambda\,|a| \leq 1$$

for all values of $n \leq 2$. The second definition has been recommended for explicit, time-accurate solutions [9, 10].

To formulate the FCT in a similar form, simply change the specification of the limiter. The traditional limiter used with the FCT is effectively a cell-edged flux rather than a cell-centered flux as needed for the modified-flux formulation. The definition of the antidiffusive flux must also be changed to a form more amenable to this formulation. This requires a more thoughtful statement of the antidiffusive flux, which can be easily incorporated with the type of formulation desired. For instance, the second-order central difference antidiffusive flux is

$$\hat{f}^{AD}_{j+\frac{1}{2}} = \frac{1}{2}\psi\left(a_{j+\frac{1}{2}}\right)\Delta_{j+\frac{1}{2}}u , \tag{34}$$

or a Lax-Wendroff flux

$$\hat{f}^{AD}_{j+\frac{1}{2}} = \frac{1}{2}\left[\psi\left(a_{j+\frac{1}{2}}\right) - \lambda a^2_{j+\frac{1}{2}}\right]\Delta_{j+\frac{1}{2}}u , \tag{35}$$

or a fourth-order central difference

$$\hat{f}^{AD}_{j+\frac{1}{2}} = \frac{1}{2}\psi\left(a_{j+\frac{1}{2}}\right)\Delta_{j+\frac{1}{2}}u + \frac{1}{12}\left(\Delta_{j-\frac{1}{2}}f - \Delta_{j+\frac{3}{2}}f\right) , \tag{36}$$

which can be written

$$\hat{f}^{AD}_{j+\frac{1}{2}} = \frac{1}{2}\psi\left(a_{j+\frac{1}{2}}\right)\Delta_{j+\frac{1}{2}}u + \frac{1}{12}\left(a_{j-\frac{1}{2}}\Delta_{j-\frac{1}{2}}u - a_{j+\frac{3}{2}}\Delta_{j+\frac{3}{2}}u\right) .$$

These forms can be incorporated with a new limiter that has the desired properties. These properties are the centering of the flux about grid point

j, and being TVD for second-order antidiffusive fluxes. This limiter has the following form:

$$g_j = \text{minmod}\left(\hat{f}^{AD}_{j\pm\frac{1}{2}}, \Delta_{j\pm\frac{1}{2}}u; n\right) = S_{j+\frac{1}{2}} \quad \max\left[0, \min\left(\frac{1}{2}n\left|\hat{f}^{AD}_{j+\frac{1}{2}}\right|, nS_{j+\frac{1}{2}}\sigma_{j-\frac{1}{2}}\Delta_{j-\frac{1}{2}}u\right),\right.$$
$$\left.\min\left(n\sigma_{j+\frac{1}{2}}\left|\Delta_{j+\frac{1}{2}}u\right|, \frac{1}{2}nS_{j+\frac{1}{2}}\hat{f}^{AD}_{j-\frac{1}{2}}\right)\right], \tag{37}$$

where $\sigma_{j+\frac{1}{2}}$ is defined by Eq. (32) or Eq. (33). The function $S_{j+\frac{1}{2}}$ is set to zero if the $\hat{f}_{j\pm\frac{1}{2}}$ differ in sign.

Remark 3 *It is important to note that this method does not require a diffusive first step to be successful.*

Analysis of this limiter for the second-order central-difference-based antidiffusive flux follows that of Sweby [28]. For the values of $0 \leq n \leq 2$ in Eq. (37), the resulting limiter is in the TVD region of the curves shown in Fig. 1. For the value of $n = 2$, the resulting limiter is identical to Roe's Superbee limiter [30]. Shown in this figure are the plots for $n = 1$ and $n = 1.5$; the plot for $n = 2$ is identical to the upper boundary of the second-order TVD region. The second-order TVD region is shown by the shaded region of the figure. These limiters are second-order for all n for $r \leq 1/2$ and also second-order for $r \geq 2/n$. The only limiter of this class that is always second-order is the $n = 2$ limiter. In this figure the terms r and Q are defined

$$r = \frac{\Delta_{j+\frac{1}{2}}u}{\Delta_{j-\frac{1}{2}}u},$$

and

$$Q = \frac{g_j}{\Delta_{j-\frac{1}{2}}u}.$$

2.4 Extension of FCT to Systems of Equations

The extension of the previously described methods to systems of hyperbolic conservation laws is no simple matter. We will consider the Euler equations where the vectors

$$\mathbf{U} = \begin{bmatrix} u^1 \\ u^2 \\ u^3 \end{bmatrix} = \begin{bmatrix} \rho \\ m \\ E \end{bmatrix},$$

and

$$\mathbf{F}(\mathbf{U}) = \begin{bmatrix} f^1 \\ f^2 \\ f^3 \end{bmatrix} = \begin{bmatrix} m \\ m^2/\rho + p \\ m(E+p)/\rho \end{bmatrix} ,$$

are defined for Eq. (3). Here $m = \rho u$ where u is the fluid velocity. The pressure, p, and density, ρ, are related to the energy by an equation of state (for an ideal gas),

$$p = \rho\varepsilon(\gamma - 1) \ ,$$

where $\varepsilon = E/\rho - 1/2u^2$ and γ is the ratio of specific heats for the gas in question. This will serve as an example of the implementation, but the use of the techniques discussed here is not limited to this equation set or equation of state. The FCT currently is extended to systems in the simplest fashion. Traditional implementations of the FCT take the pressure terms in F as source terms and are handled with central differences. This leads to a poor representation of the wave interactions and the results that follow are often less than satisfactory.

The use of exact and approximate Riemann solvers offers a way through which more of the physical nature of the solution can be integrated into the solution procedure. To the authors' knowledge no attempt has been made to incorporate Riemann solvers with any of the previous FCT algorithms. Using van Leer's Riemann solver [6, 31], with Godunov's first-order method [1, 32] as the low-order method with the first modification of the FCT limiter, was our first attempt to incorporate a Riemann solver with FCT. While the results are better than the standard FCT implementation, they are worse than Godunov's method alone. A second approach is detailed below using Roe's approximate Riemann solver.

Roe's approximate Riemann solver and its descendents use a decomposition of the characteristic field for the system of conservation laws. Taking the form of the system of hyperbolic conservation laws given in Eq. (4), the flux Jacobian, A, is decomposed into right and left eigenvectors and eigenvalues or characteristics as

$$A = R\Lambda R^{-1} \ , \tag{38}$$

where R is a matrix where the columns are the eigenvectors, $\mathbf{r}^k$, of the eigenvalues, a^k, which are the diagonal entries of Λ. The matrix R^{-1} is the inverse of R whose rows will be denoted as $\mathbf{l}^k$, the left eigenvectors, where the index k refers to the k^{th} wave in the system.

In Roe's formulation it is required that the matrix A is averaged from its neighboring states so that

$$(\mathbf{F}_{j+1} - \mathbf{F}_j) = A_{j+\frac{1}{2}} (\mathbf{U}_{j+1} - \mathbf{U}_j) \ .$$

This averaging for the system in question requires that a parameter be defined by

$$D_{j+\frac{1}{2}} = (\rho_{j+1}/\rho_j)^{1/2} \ , \tag{39}$$

which is in turn used to define the following cell edge values:

$$u_{j+\frac{1}{2}} = \frac{D_{j+\frac{1}{2}} u_{j+1} + u_j}{D_{j+\frac{1}{2}} + 1} \ , \tag{40}$$

$$H_{j+\frac{1}{2}} = \frac{D_{j+\frac{1}{2}} H_{j+1} + H_j}{D_{j+\frac{1}{2}} + 1} \ , \tag{41}$$

and

$$c_{j+\frac{1}{2}} = \left[(\gamma - 1) \left(H_{j+\frac{1}{2}} - \frac{1}{2} u^2_{j+\frac{1}{2}} \right) \right]^{1/2} \ , \tag{42}$$

where

$$H = \frac{\gamma p}{(\gamma - 1)\rho} + \frac{1}{2} u^2 \ . \tag{43}$$

For the Euler equations, the eigenvalues of the flux Jacobian are

$$\left(a^1, a^2, a^3 \right) = (u, u + c, u - c) \ . \tag{44}$$

The right eigenvectors form a matrix

$$R = \left(\mathbf{r}^1, \mathbf{r}^2, \mathbf{r}^3 \right) = \begin{bmatrix} 1 & 1 & 1 \\ u & u + c & u - c \\ \frac{1}{2} u^2 & H + uc & H - uc \end{bmatrix} \ , \tag{45}$$

and by using

$$z_1 = \frac{1}{2} (\gamma - 1) \frac{u^2}{c^2} \ ,$$

$$z_2 = \frac{\gamma - 1}{c^2} \ ,$$

the left eigenvectors form a matrix

$$R^{-1} = \begin{bmatrix} \mathbf{l}^1 \\ \mathbf{l}^2 \\ \mathbf{l}^3 \end{bmatrix} = \begin{bmatrix} 1 - z_1 & z_2 u & -z_2 \\ \frac{1}{2}\left(z_1 - \frac{u}{c}\right) & -\frac{1}{2}\left(z_2 u - \frac{1}{c}\right) & \frac{1}{2} z_2 \\ \frac{1}{2}\left(z_1 + \frac{u}{c}\right) & -\frac{1}{2}\left(z_2 u + \frac{1}{c}\right) & \frac{1}{2} z_2 \end{bmatrix} . \tag{46}$$

In the results presented in the next section, Roe's [20] averaging procedure was used.

The implementation of these Riemann solvers relies on the following transformations:

$$\Delta_{j+\frac{1}{2}} u^j = \sum_k r^k_{j+\frac{1}{2}} \alpha^k_{j+\frac{1}{2}} , \tag{47}$$

where

$$\alpha^k_{j+\frac{1}{2}} = \sum_j l^k_{j+\frac{1}{2}} \Delta_{j+\frac{1}{2}} u^j . \tag{48}$$

The numerical dissipation terms are then written as

$$\Phi^{DC}_{j+\frac{1}{2}} = \sum_k \frac{1}{2} r^k_{j+\frac{1}{2}} \psi\left(a^k_{j+\frac{1}{2}}\right) \alpha^k_{j+\frac{1}{2}} , \tag{49}$$

$$\Phi^{FCT}_{j+\frac{1}{2}} = \sum_k r^k_{j+\frac{1}{2}} \left(f^{C\,k}_{j+\frac{1}{2}} + \Phi^{DC}_{j+\frac{1}{2}} \right) , \tag{50}$$

and

$$\Phi^{MF}_{j+\frac{1}{2}} = \sum_k \frac{1}{2} r^k_{j+\frac{1}{2}} \left[g^k_j + g^k_{j+1} - \psi\left(a^k_{j+\frac{1}{2}} + \gamma^k_{j+\frac{1}{2}}\right) \alpha^k_{j+\frac{1}{2}} \right] , \tag{51}$$

where

$$g^k_j = \operatorname{minmod}\left(\sigma^k_{j-\frac{1}{2}} \alpha^k_{j-\frac{1}{2}}, \sigma^k_{j+\frac{1}{2}} \alpha^k_{j+\frac{1}{2}} \right) , \tag{52}$$

and

$$\gamma^k_{j+\frac{1}{2}} = \begin{cases} \dfrac{\Delta_{j+\frac{1}{2}} g^k}{\alpha^k_{j+\frac{1}{2}}} & \text{if } \alpha_{j+\frac{1}{2}} \neq 0 \\ 0 & \text{otherwise} \end{cases} . \tag{53}$$

Given these expressions for the numerical dissipation, the flux limiters used in the modified FCT (and for that matter classical FCT) Eqs. (11),(13), and (37) are rewritten to take advantage of these forms. When a monotone first step is required with the FCT, Roe's first-order method [20] plus the entropy correction is used for the low- order method. The antidiffusive fluxes for the k^{th} wave are rewritten as

$$\hat{f}^{AD}_{j+\frac{1}{2}} = \frac{1}{2}\psi\left(a^k_{j+\frac{1}{2}}\right)\alpha^k_{j+\frac{1}{2}} \ , \tag{54}$$

or a Lax-Wendroff flux

$$\hat{f}^{AD}_{j+\frac{1}{2}} = \frac{1}{2}\left[\psi\left(a^k_{j+\frac{1}{2}}\right) - \lambda\left(a^k_{j+\frac{1}{2}}\right)^2\right]\alpha^k_{j+\frac{1}{2}} \ , \tag{55}$$

or a fourth-order central difference

$$\hat{f}^{AD}_{j+\frac{1}{2}} = \frac{1}{2}\psi\left(a^k_{j+\frac{1}{2}}\right)\alpha^k_{j+\frac{1}{2}} + \frac{1}{12}\left(a^k_{j-\frac{1}{2}}\alpha^k_{j-\frac{1}{2}} - a^k_{j+\frac{3}{2}}\alpha^k_{j+\frac{3}{2}}\right) \ . \tag{56}$$

For the classic FCT method, the flux limiter becomes

$$\hat{f}^{C}_{j+\frac{1}{2}} = S_{j+\frac{1}{2}} \max\left[0, \min\left(S_{j+\frac{1}{2}}\lambda^{-1}\alpha^k_{j-\frac{1}{2}}, \left|\hat{f}^{AD}_{j+\frac{1}{2}}\right|, S_{j+\frac{1}{2}}\lambda^{-1}\alpha^k_{j+\frac{3}{2}}\right)\right] \ . \tag{57}$$

The new FCT limiter becomes

$$\hat{f}^{C\,k}_{j+\frac{1}{2}} = S_{j+\frac{1}{2}} \max\left[0, \min\left(S_{j+\frac{1}{2}}\tilde{\sigma}^k_{j-\frac{1}{2}}\tilde{\alpha}^k_{j-\frac{1}{2}}, \left|\hat{f}^{AD}_{j+\frac{1}{2}}\right|, S_{j+\frac{1}{2}}\tilde{\sigma}^k_{j+\frac{3}{2}}\tilde{\alpha}^k_{j+\frac{3}{2}}\right)\right] \ , \tag{58}$$

where

$$\tilde{\sigma}^k_{j+\frac{1}{2}} = \psi\left(\tilde{a}^k_{j+\frac{1}{2}}\right)$$

or

$$\tilde{\sigma}^k_{j+\frac{1}{2}} = \psi\left(\tilde{a}^k_{j+\frac{1}{2}}\right) - \lambda\left(a^k_{j+\frac{1}{2}}\right)^2 \ .$$

The modified-flux FCT method becomes

$$\begin{aligned} g_j = \operatorname{minmod}\left(\hat{f}^{AD}_{j\pm\frac{1}{2}}, \Delta_{j\pm\frac{1}{2}}\alpha; n\right) = S_{j+\frac{1}{2}} \quad & \max \quad \Big[\ 0, \min\left(\frac{1}{2}n\left|\hat{f}^{AD}_{j+\frac{1}{2}}\right|, nS_{j+\frac{1}{2}}\sigma_{j-\frac{1}{2}}\alpha^k_{j-\frac{1}{2}}\right), \\ & \min \quad \left(n\sigma_{j+\frac{1}{2}}\left|\alpha^k_{j+\frac{1}{2}}\right|, \frac{1}{2}nS_{j+\frac{1}{2}}\hat{f}^{AD}_{j-\frac{1}{2}}\right)\ \Big] \ , \end{aligned} \tag{59}$$

where

$$\sigma^k_{j+\frac{1}{2}} = \frac{1}{2}\psi\left(a^k_{j+\frac{1}{2}}\right)$$

or

$$\sigma^k_{j+\frac{1}{2}} = \frac{1}{2}\left[\psi\left(a^k_{j+\frac{1}{2}}\right) - \lambda\left(a^k_{j+\frac{1}{2}}\right)^2\right] \ .$$

In the next section, we will discuss the quality of solutions using these methods.

3 Results

To gauge the capability of the methods discussed in the previous sections, three test problems were solved with the FCT methods and several other high-resolution finite-difference methods. The other methods used will not be described in detail here. The first test problem will be to solve a scalar advection equation, Eq. (1), on a uniform grid. Two problems will be considered: a square wave and a sine wave over a complete period. Both waves have an amplitude of one. The second problem will be the inviscid Burger's equation,

$$\frac{\partial u}{\partial t} + \frac{\partial}{\partial x}\left(\frac{1}{2}u^2\right) = 0 \ ,$$

with initial data of a sine wave on a periodic domain with an amplitude of one. This solution will be compared with the exact solution and the corresponding error norms will be used to show convergence and order of approximation in these norms for the various methods. Finally, the shock tube problem used by Sod [32] will be used as a vehicle for comparison of these methods for their use with systems of hyperbolic conservation laws.

3.1 Scalar Advection Equation

For the scalar advection of a square wave with a uniform velocity, the FCT performs quite well with very little numerical diffusion present in the solution. These solutions are obtained for a CFL number held constant at 1/2 after 80 time steps.

As shown in Fig. 2 (a), the square wave is captured quite well by the difference scheme, however, there is a distinct lack of symmetry in the solution. This lack of symmetry is evident in this version of the FCT despite the choice of the CFL number (which should lead to symmetric results, ideally because of the phase error properties of upwind methods at a CFL number of $\frac{1}{2}$ [33]). The lack of symmetry can be attributed to the support of the limiter, which can result in anti-upwind data being used in the flux definition [34]. This is more evident in Fig. 2 (b), but also evident is the overcompressive nature of the scheme. The sine wave is in the process of being compressed into two square waves. This behavior is clearly unacceptable because the character of the waves is largely destroyed by this algorithm. Figure 3 shows that the new FCT algorithm is somewhat more diffusive (less compressive) and has the more of the expected symmetry in the solution. Figure 3 (b) still shows that this algorithm remains too compressive despite being TVD. One negative aspect of this calculation is the clipping of the extrema with respect to the previous figure, although overall this solution is superior in most respects to Zalesak's FCT.

By using the Lax-Wendroff fluxes as the base for the antidiffusive fluxes, the problem of overcompression is eliminated from both algorithms. This is at the cost of some clipping of the solution's extrema. The clipping in Fig. 4 is less than that in Fig. 5, but at the cost of the symmetry of the solution. The lack of symmetry is also present in these results.

Figures 6 and 7 show the impact of the choice of n in the modified-flux FCT formulation (and for that matter other implementations of limiters). Here the Lax-Wendroff based high-order fluxes are used. The lower value of n results in solutions that exhibit a great deal of dissipation and clipping of extrema. For the $n = 2$, solution is of high quality with the clipping of extrema quite controlled. This solution nearly equals that of the other FCT formulations for the square wave. For the sine wave, despite some clipping, the overcompression has disappeared with the character of the original profile well preserved.

The symmetric TVD algorithm (second-order in both time and space) produces results similar to the new FCT, but with a lack of symmetry. This can be cured with a predictive first step as with the FCT. As Fig. 8 shows, both exhibit a fair amount of extrema clipping and lack of symmetry. These are similar to the results obtained in Fig. 4 with Zalesak's FCT, but are more diffused.

3.2 Burger's Equation

In all cases, the solutions obtained by using the high-resolution algorithms on Burger's equation are quite good in terms of quality. Little would be gained by simply viewing their profiles (they are similar to the results in [10] for a TVD algorithm). By nature these high-resolution methods produce results that are first-order accurate in the L_∞ norm and approach second-order accuracy in the L_1 norm. In the next four figures discussed, figure (a) will be for time equal to 0.2 when the solution remains smooth, and (b) will show the error norms (L_1, L_2 and L_∞) at time equal 1.0 after a shock has formed. For the methods used, each is second-order in time and space with the exception of the fourth-order FCT method, which is fourth-order in space. Second-order temporal accuracy is obtained by using a Lax-Wendroff type formulation. These calculations are all done with λ held constant. The norms shown in the figures are defined as follows:

$$L_1 = \sum_j^N \frac{|e_j|}{N} \ ,$$

$$L_2 = \left(\sum_j^N \frac{e_j^2}{N} \right)^{\frac{1}{2}} \ ,$$

$$L_\infty = \sup \left(|e_j| \right) \ ,$$

where

$$e_j = U_j^{exact} - U_j^{approx.} \ .$$

In Fig. 9 the solution for $t = 0.2$ converges in the expected fashion, but at $t = 1$ problems are present with the convergence in the L_∞ norm. As the grid is refined, the L_∞ norm error increases rather than decreases as expected. As the grid size is further decreased convergence resumes, but is quite slow (about order 1/4). Figure 10 shows that the convergence properties of the fourth-order antidiffusive flux do not converge at a fourth-order rate and are in fact worse than those shown in the previous figure. The nonconvergence in the L_∞ norm for intermediate grid sizes for the $t = 1$ case is comparable. The new FCT algorithm shows slight improvements over both of these cases, but still has the same difficulties after a shock has formed in the solution. As shown by Fig. 11, the solutions converge faster than Zalesak's FCT, but are still plagued by some of the same problems. This behavior is also shared by the symmetric TVD's results in Fig. 12. The symmetric TVD does not converge as well as the new FCT method, but the nonconvergence problem is not as pronounced although it is clearly present.

The similarity of the solutions for the two FCT methods and the symmetric TVD algorithm, and the lack of such a problem in the modified-flux FCT (or TVD) method points to the form of the limiter as being the problem. The FCT and symmetric TVD use cell-edged limiters rather than cell-centered limiters. This difference requires that each limiter has a wider spatial stencil than the cell-centered limiter, and as a result the resulting algorithm is not as sensitive to the presence of a discontinuity. This lack of sensitivity results in a poorer handling of shocks and discontinuities. The FCT is less diffusive than the symmetric TVD method, and this lack of diffusion increases the problem. The results for the fourth-order spatial limiter point out two problems: because the fourth-order spatial difference is more compressive than the second-order difference scheme, the convergence difficulty in the L_∞ norm at a shock is increased slightly. Experiments with a second-order Runge-Kutta time integration scheme show improvements in the L_1 convergence of the FCT.

3.3 Sod's Shock Tube Problem

The third problem involves the solution of Sod's test problem which tests the mettle of each algorithm against a difficult physical problem. For the FCT methods [in the modified-flux $\sigma = 1/2\left(|a| - \lambda a^2\right)$], the Lax-Wendroff flux is used to define the antidiffusive flux. All results were produced for $\Delta t = 0.4\Delta x$ and shown for $t = 0.24$. The initial conditions are the same as Sod uses, but are listed here for completeness, for $X < 0.5$,

$$\begin{bmatrix} \rho^l \\ u^l \\ p^l \end{bmatrix} = \begin{bmatrix} 1.0 \\ 0.0 \\ 1.0 \end{bmatrix},$$

and for $X \geq 0.5$

$$\begin{bmatrix} \rho^r \\ u^r \\ p^r \end{bmatrix} = \begin{bmatrix} 0.125 \\ 0.0 \\ 0.1 \end{bmatrix},$$

with $\gamma = 1.4$.

Figure 13 shows that the results using Zalesak's FCT are reasonable, but are polluted with a fair number of nonlinear instabilities. These instabilities are significantly worse if the limiter is based on a second-order central differences with numerous small expansion shocks present in the rarefaction fan. Even with the extra diffusion produced by the Lax-Wendroff flux, an expansion shock is present in the rarefaction wave and oscillations are present in the preshock region of the flow. The overall quality of this solution is quite poor. The new FCT formulation produces qualitatively better results that appear to be due to greater dissipation in the scheme. The expansion shock is no longer present. The overall quality of this solution is not high because of the considerable smearing of the features of the flow. In Fig. 14, the results show that a great deal of smearing is present except at the shock wave where the solution is very sharp. In both of these figures the pressure-related terms in the momentum and energy equations are incorporated as source terms rather than as convective fluxes, and are central differenced.

By computing the first step of the new FCT with Roe's first-order scheme, and using an approximate Riemann solver to compute the flux correction, the results are extremely good. As Fig. 15 shows, the smearing of a standard FCT implementation of the new FCT is gone, with the shock being computed with the same crispness. The rarefaction fan is smooth and in good agreement with the exact solution. The resolution of the contact discontinuity is somewhat smeared but is acceptable.

The modified-flux FCT (Fig. 16) has slightly poorer resolution of the contact discontinuity, but computes the shock in a sharper fashion. The overall quality of the solution is nearly identical to the previous case. In this case the value of $n = 1.5$ was used on all three fields. Better resolution of the contact discontinuity could be obtained with the $n = 2$ limiter. The use of the $n = 2$ limiter with the nonlinear fields is generally ill-advised [28]. The final two figures are shown for comparison with the previous figures. The symmetric TVD method (Fig. 17), gives adequate solution although the amount of smearing exceeds that of the other methods incorporating Roe's approximate Riemann solver. The UNO method (implemented with a method similar to the modified-flux TVD algorithm [8, 35]) was used to compute the solution shown in Fig. 18. This solution is of a quality similar to that found in Fig. 16 with slightly better resolution of each of the features of the flow. Issues related to limiter construction in FCT may need additional work to improve the results found using new FCT algorithms. It is not clear that simply using higher order antidiffusive fluxes will yield better results near extrema and discontinuities in the solution without improvements in the other terms in the limiter.

4 Concluding Remarks

A generalized FCT algorithm is shown to be TVD under certain conditions. The method does not need the standard diffusive first step in older FCT algorithms. The new algorithm has improved properties from the standpoint of both use and analysis. Results show that the new FCT algorithms (both "new FCT" and modified-flux FCT) perform better than the older FCT algorithms, and are comparable with other modern methods. This is shown to be especially important for systems of equations where the improvement is greater than with the scalar wave equation. The new formulation allows Riemann solvers to be used effectively with FCT methods. Additionally, this paper has more clearly defined the link between FCT methods and TVD methods. This will allow advances made with one method to more easily fertilize improvements in the other type of method.

The initial motivation of this work was to tie together in a more coherent fashion the various modern high-resolution methods for numerically solving hyperbolic conservation laws. This work should be considered a start, with the advances mentioned above, as progress toward this goal.

Future work will include the modification of the FCT to include MUSCL-type schemes as well as the appropriate generalization of Zalesak's multi-dimensional limiter to these types of methods. As mentioned earlier, these methods, once cast in the appropriate form, can be used for implicit time integration where the necessary form is similar to that found in TVD implicit formulations. Tests on simple test problems indicate that these methods are unconditionally stable.

In the next paper of this series we will extend the current analysis to a more geometric approach.

Acknowledgments

This work was performed under the auspices of the U. S. Department of Energy.

References

[1] S. K. Godunov. Finite difference method for numerical computation of discontinuous solutions of the equations of fluid dynamics. *Matematicheski Sbornik*, 47:271–306, 1959.

[2] J. P. Boris and D. L. Book. Flux-corrected transport I. SHASTA, a fluid transport algorithm that works. *Journal of Computational Physics*, 11:38–69, 1973.

[3] J. P. Boris, D. L. Book, and K Hain. Flux-corrected transport II: Generalizations of the method. *Journal of Computational Physics*, 18:248–283, 1975.

[4] J. P. Boris and D. L. Book. Flux-corrected transport III. minimal-error FCT algorithms. *Journal of Computational Physics*, 20:397–431, 1976.

[5] J. P. Boris and D. L. Book. *Solution of Continuity Equations by the Method of Flux- Corrected Transport*, volume 16, pages 85–129. Academic Press, 1976.

[6] B. van Leer. Towards the ultimate conservative difference scheme. V. A second-order sequel to Godunov's method. *Journal of Computational Physics*, 32:101–136, 1979.

[7] A. Harten and S. Osher. Uniformly high-order accurate nonoscillatory schemes. I. *SIAM Journal on Numerical Analysis*, 24:279–309, 1987.

[8] A. Harten, B. Engquist, S. Osher, and S. Chakravarthy. Uniformly high order accurate essentially non-oscillatory schemes, III. *Journal of Computational Physics*, 71:231–303, 1987.

[9] A. Harten. On a class of high resolution total-variation-stable finite-difference schemes. *SIAM Journal on Numerical Analysis*, 21:1–23, 1984.

[10] H. C. Yee, R. F. Warming, and A. Harten. Implicit total variation diminishing (TVD) schemes for steady-state applications. *Journal of Computational Physics*, 57:327–360, 1985.

[11] B. van Leer. Upwind-difference methods for aerodynamic problems governed by the Euler equations. In B. Engquist et al., editor, *Lectures in Applied Mathematics*, volume 22, pages 327–336, 1985.

[12] H. C. Yee, G. H. Klopfer, and J.-L. Montagne. High-resolution shock-capturing schemes for inviscid and viscous hypersonic flows. *Journal of Computational Physics*, 88:31–61, 1990.

[13] S. T. Zalesak. Fully multidimensional flux-corrected transport algorithms for fluids. *Journal of Computational Physics*, 31:335–362, 1979.

[14] B. E. McDonald. Flux-corrected pseudospectral method for scalar hyperbolic conservation laws. *Journal of Computational Physics*, 82:413–428, 1989.

[15] P. Steinle and R. Morrow. An implicit flux-corrected transport algorithm. *Journal of Computational Physics*, 80:61–71, 1989.

[16] R. Löhner, K. Morgan, J. Peraire, and M. Vahdati. Finite element flux-corrected transport (FEM-FCT) for the Euler and Navier-Stokes equations. *International Journal for Numerical Methods in Fluids*, 7:1093–1109, 1987.

[17] T. Ikeda and T. Nakagawa. On the SHASTA FCT algorithm for the equation $\partial\rho/\partial t + \partial\left(v\left(\rho\right)\right)/\partial x = 0$. *Mathematics of Computation*, 33:1157–1169, 1979.

[18] P. Woodward and P. Colella. The numerical simulation of two-dimensional fluid flow with strong shocks. *Journal of Computational Physics*, 54:115–173, 1984.

[19] S. T. Zalesak. High order "ZIP" differencing of convective terms. *Journal of Computational Physics*, 40:497–508, 1981.

[20] P. L. Roe. Approximate Riemann solvers, parameter vectors, and difference schemes. *Journal of Computational Physics*, 43:357–372, 1981.

[21] P. D. Lax. *Hyperbolic Systems of Conservation Laws and the Mathematical Theory of Shock Waves*. SIAM, 1972.

[22] J. Smoller. *Shock Waves and Reaction-Diffusion Equations*. Springer-Verlag, 1982.

[23] H. C. Yee. Construction of explicit and implicit symmetric TVD schemes and their applications. *Journal of Computational Physics*, 68:151–179, 1987.

[24] A. Harten, P. D. Lax, and B. van Leer. On upstream differencing and Godunov-type schemes for hyperbolic conservation laws. *SIAM Review*, 25:35–61, 1983.

[25] B. Engquist and S. Osher. One-sided difference approximations for nonlinear conservation laws. *Mathematics of Computation*, 36:321–351, 1981.

[26] E. S. Oran and J. P. Boris. *Numerical Simulation of Reactive Flow*. Elsiver, 1987.

[27] S. T. Zalesak. A preliminary comparison of modern shock-capturing schemes: Linear advection. In R. Vichnevetsky and R. S. Stepleman, editors, *Advances in Computer Methods for Partial Differential Equations*, volume 6, pages 15–22. IMACS, 1987.

[28] P. K. Sweby. High-resolution schemes using flux limiters for hyperbolic conservation laws. *SIAM Journal on Numerical Analysis*, 21:995–1011, 1984.

[29] H. C. Yee. Upwind and symmetric shock-capturing schemes. Technical Report NASA TM–89464, NASA, 1987.

Figure 1: The characteristics of the FCT limiters for the modified-flux formulation.

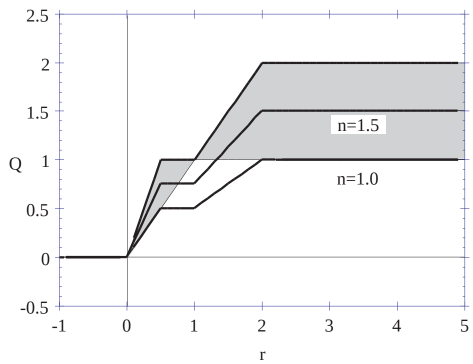

[30] P. L. Roe. Some contributions to the modelling of discontinuous flows. In B. Engquist et al., editor, *Lectures in Applied Mathematics*, volume 22, pages 163–193, 1985.

[31] J. J. Gottlieb and C. P. T. Groth. Assessment of Riemann solvers for unsteady one-dimensional inviscid flows of perfect gases. *Journal of Computational Physics*, 78:437–458, 1988.

[32] G. Sod. A survey of several finite difference methods for systems of nonlinear hyperbolic conservation laws. *Journal of Computational Physics*, 27:1–31, 1978.

[33] C. Hirsch. *Numerical Computation of Internal and External Flows: Volume 1*. Wiley-Interscience, 1988.

[34] W. J. Rider. A comparison of TVD Lax-Wendroff schemes. Technical Report LA–UR–91–2770, Los Alamos National Laboratory, 1992. Accepted in Communications in Applied Numerical Methods.

[35] C.-D. Munz. On the numerical dissipation of high resolution schemes for hyperbolic conservation laws. *Journal of Computational Physics*, 77:18–39, 1988.

Figure 2: Solution of the scalar advection equation with Zalesak's FCT with the high-order flux defined by second-order central differencing.

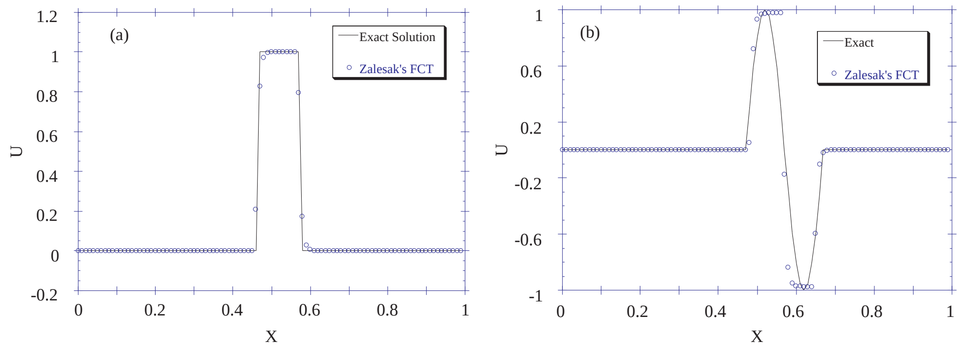

Figure 3: Solution of the scalar advection equation with the new FCT with the high-order flux defined by second-order central differencing.

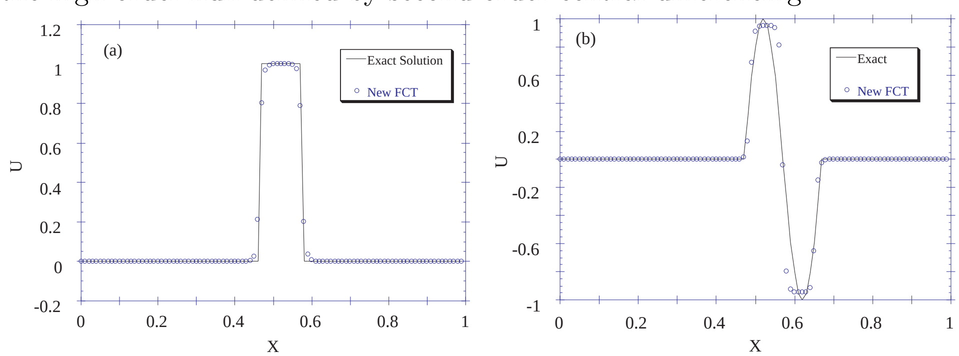

Solution of the scalar advection equation with Zalesak's FCT with the high-order flux defined by Lax-Wendroff differencing.

Figure 4:

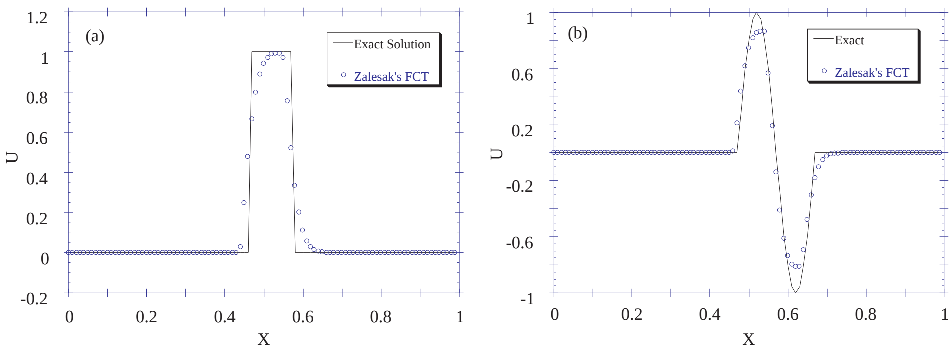

Figure 5: Solution of the scalar advection equation with the new FCT with the high-order flux defined by Lax-Wendroff differencing.

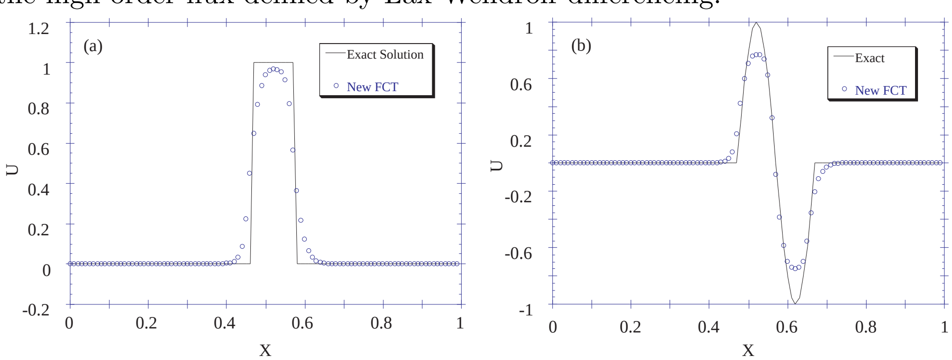

Figure 6: Solution of the scalar advection equation with the modified-flux FCT ($n = 1$ limiter).

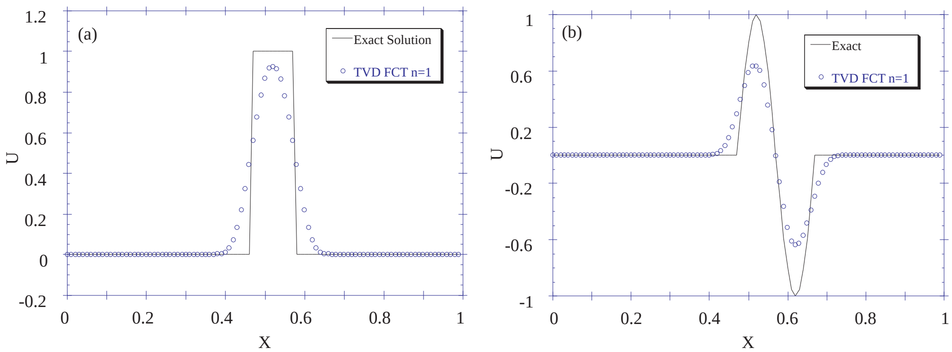

Figure 7: Solution of the scalar advection equation with the modified-flux FCT ($n = 2$ limiter).

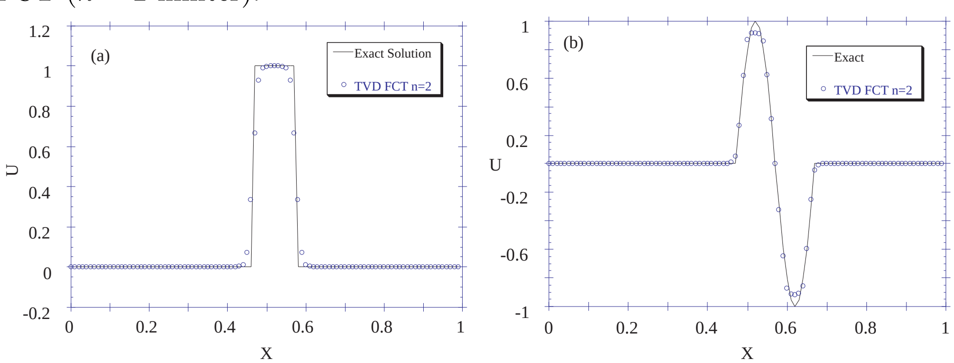

Figure 8: Solution of the scalar advection equation with a symmetric TVD scheme.

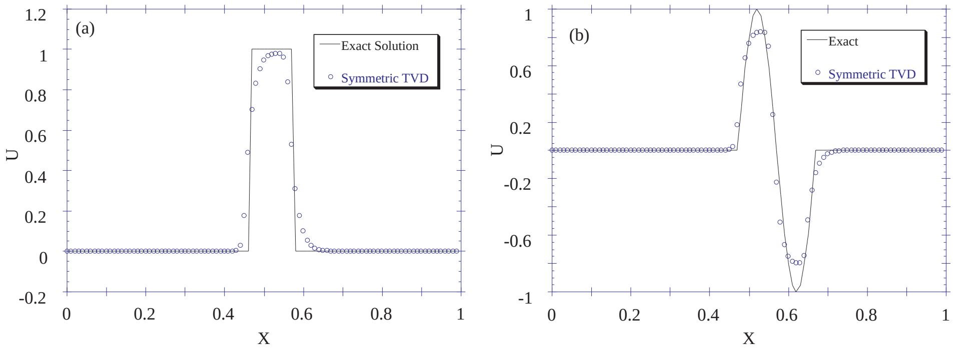

Figure 9: Convergence of error norms for Burger's equation for Zalesak's FCT with the high-order flux defined by Lax-Wendroff differencing.

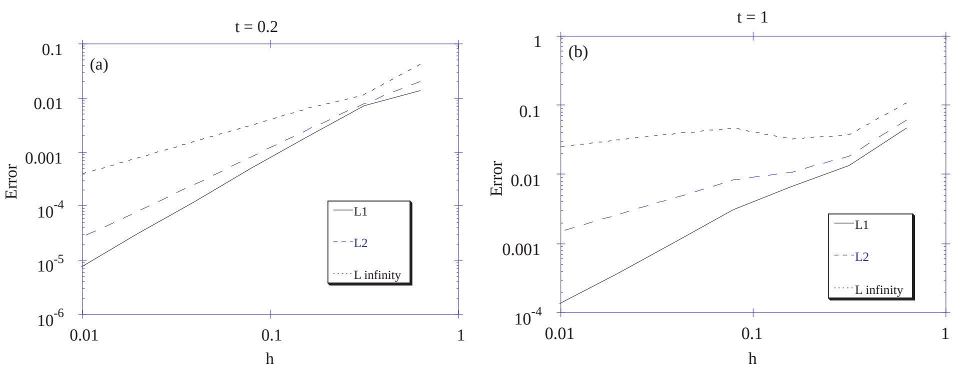

Figure 10: Convergence of error norms for Burger's equation for Zalesak's FCT with the high-order flux defined by fourth-order central differencing.

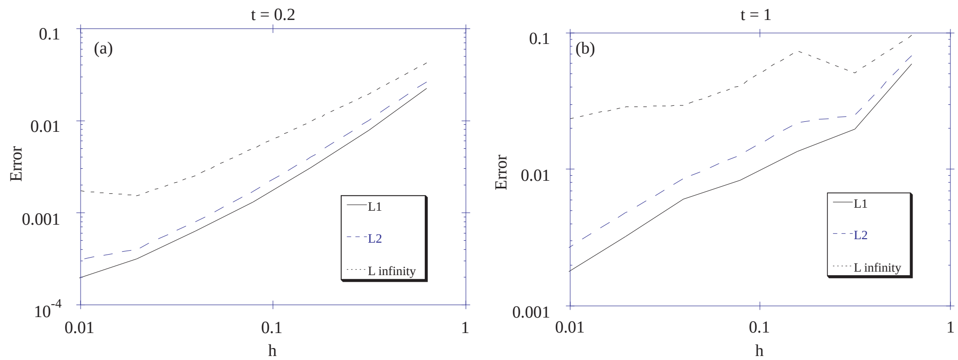

Figure 11: Convergence of error norms for Burger's equation for the new FCT with the high-order flux defined by Lax-Wendroff differencing.

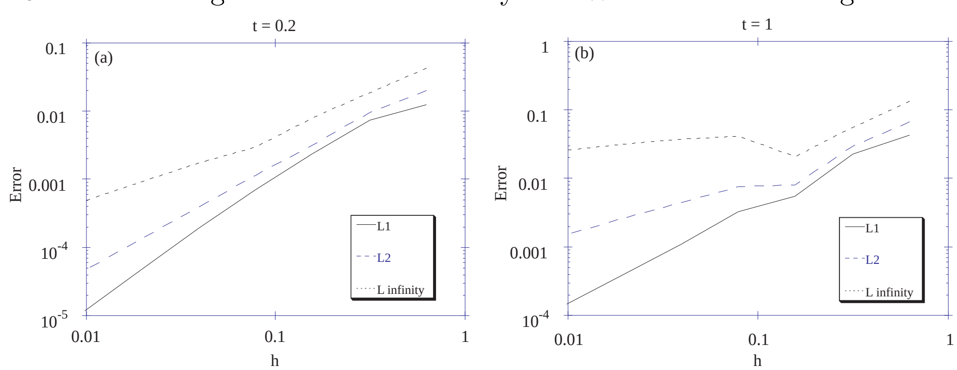

Figure 12: Convergence of error norms for Burger's equation for a symmetric TVD algorithm.

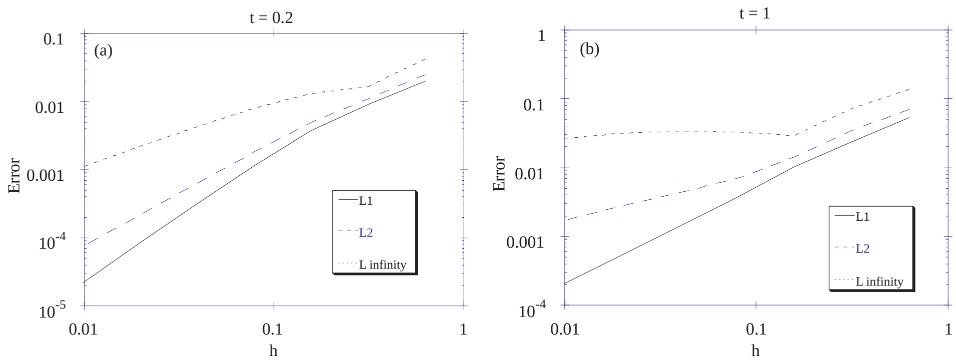

Figure 13: Solution of Sod's shock tube problem with Zalesak's FCT.

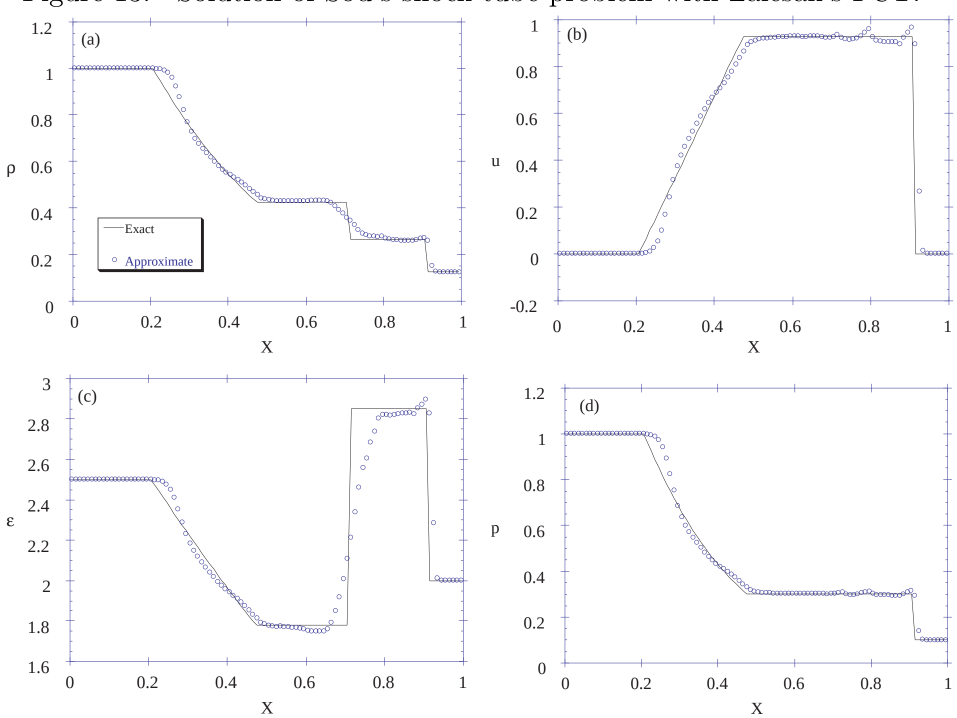

Figure 14: Solution of Sod's shock tube problem with the new FCT.

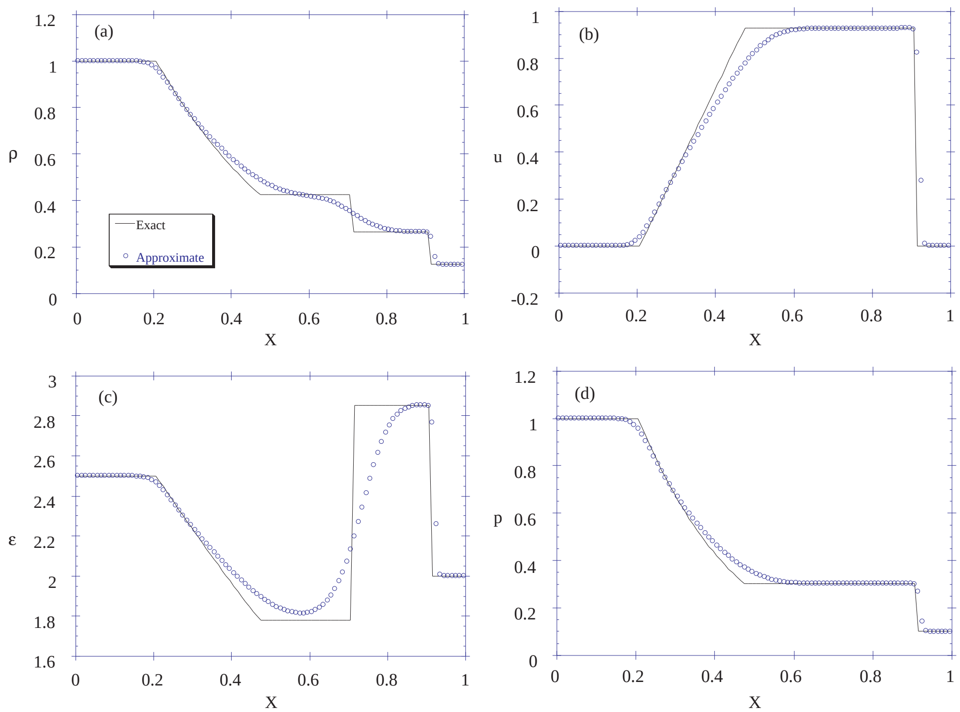

Figure 15: Solution of Sod's shock tube problem with new FCT with Roe's approximate Riemann solver used to define both low- and high-order fluxes.

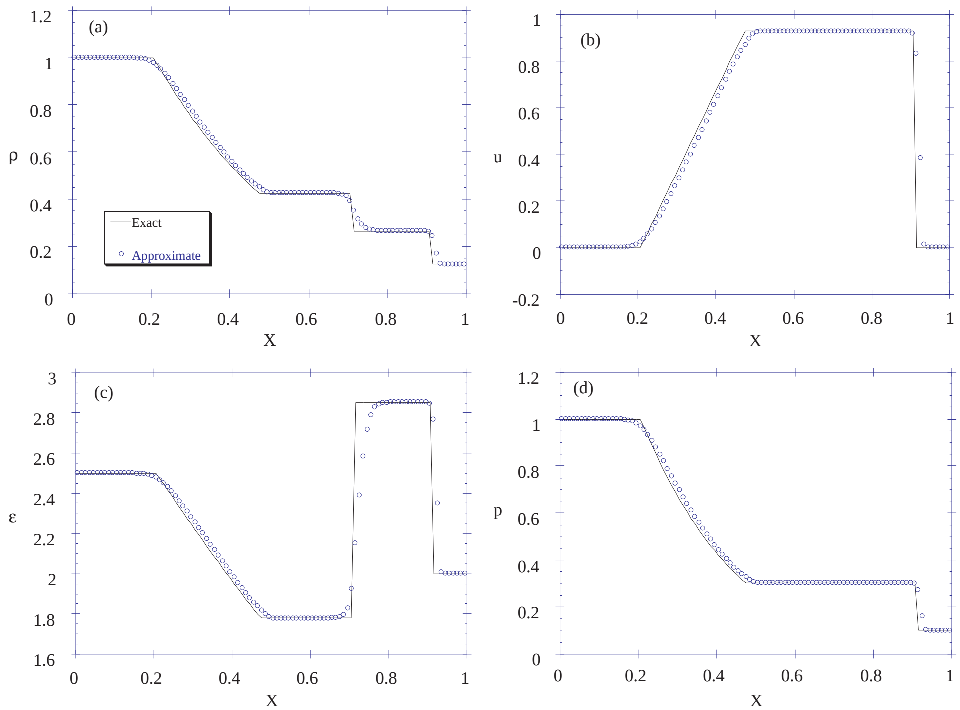

Figure 16: Solution of Sod's shock tube problem with the modified-flux FCT and $n = 1.5$ limiters on all fields.

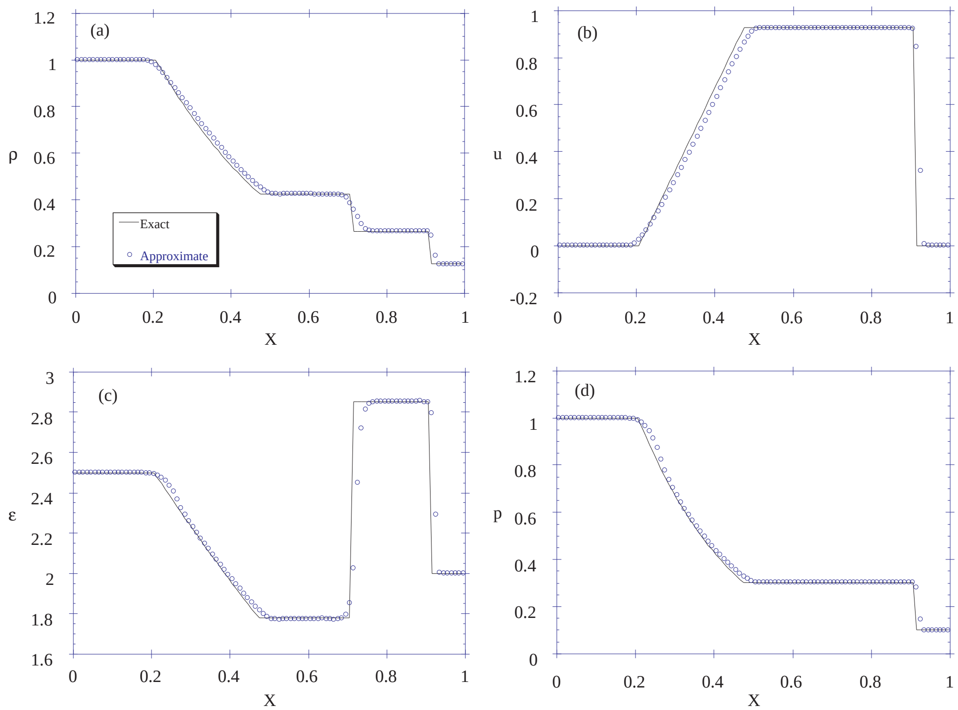

Figure 17: Solution of Sod's shock tube problem with a symmetric TVD algorithm.

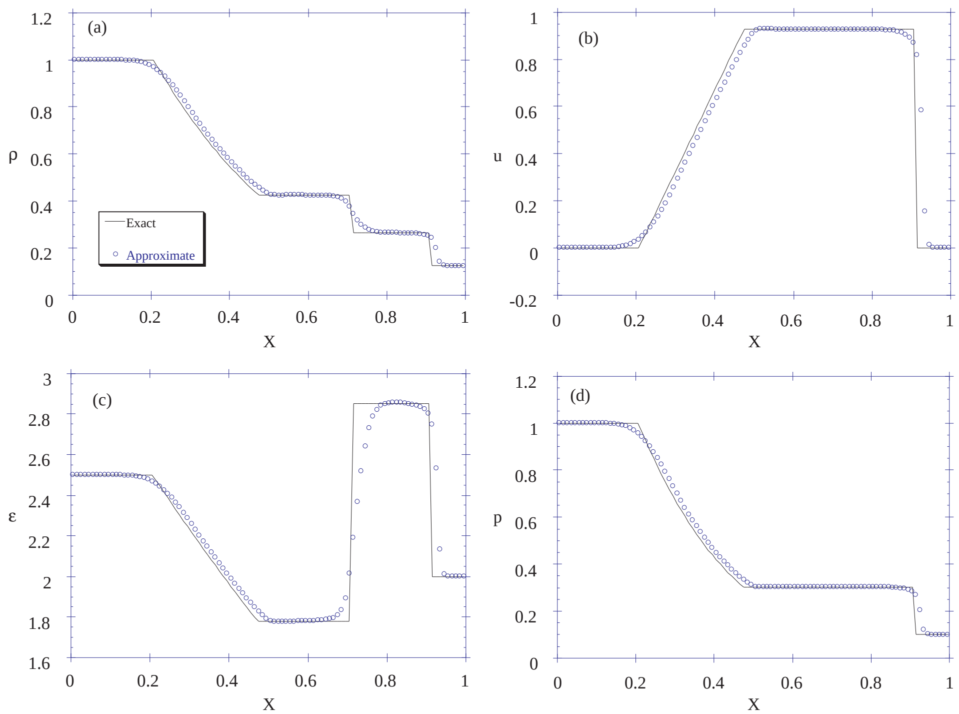

Figure 18: Solution of Sod's shock tube problem with a UNO limiter and a modified-flux TVD algorithm.